

# Light and Electron Microscopic Study on the Possible Ameliorative Role of Adipose-Derived Mesenchymal Stem Cells on Diabetic Retinopathy in Adult Male Albino Rats

Original  
Article

Magdy F. Gawish, Nehad F. Mazen, Ebtehal Z. Hassen and Mai E. Adbelhady

Department of Histology and Cell Biology, Faculty of Medicine, Zagazig University

## ABSTRACT

**Introduction:** Stem cell-based therapies have the potential effectivity in many human diseases including retinal disorders. They have been proven to be safe and effective in a wide range of immune-mediated diseases.

**Aim of the work:** To investigate the effectiveness of ADMSCs in the prevention of retinal damage after induction of diabetes.

**Material and methods:** Forty adult male rats were divided into three groups; Group I: subdivided into negative and positive control. Group II: received a single intraperitoneal injection of STZ (50 mg/kg), freshly dissolved in 0.9% saline solution. Blood glucose levels were measured two days after STZ injection, and rats with glucose levels  $\geq 250$  mg/dl were considered diabetic and used in the study. Group III: received STZ, in the same previous dose, then the diabetic rats were injected intravenously with 0.5 ml ADMSCs ( $1 \times 10^7$  cells/ml) suspended in phosphate-buffered saline. After four weeks, retinal specimens were prepared for histological and immunohistochemical studies.

**Results:** The retina of STZ-treated group showed poorly-developed basal infoldings of RPE cells, distorted lamellar discs of photoreceptor outer segments, loss of cellular elements in the outer nuclear layer, inner nuclear layer and ganglion cell layer, and apoptosis. After ADMSCs administration, there was improvement in the retinal structure. There was highly significant decrease in the area percent of caspase-3 in cells of all retinal layers, compared to the diabetic group, and no difference was found when compared with the control group.

**Conclusion:** ADMSCs was proved to be effective in the prevention of retinopathy in experimentally-induced diabetic rat model. This might represent a valuable tool for stem cell-based therapy in the future.

**Received:** 11 June 2018, **Accepted:** 21 September 2018

**Key Words:** Adipose-derived mesenchymal stem cells, caspase-3, diabetes, rat, retina.

**Corresponding Author:** Ebtehal Z. Hassen, M.D, Department of Histology and Cell Biology, Faculty of Medicine, Zagazig University, **Tel.:** +2 1001244853, **E-mail:** ebtehalzaid.81@gmail.com

**ISSN:** 1110-0559, Vol. 41, No. 4

## INTRODUCTION:

Diabetes mellitus has reached the state of an epidemic in developed countries and in the developing ones; the incidence of diabetes is increasing at still a quicker pace<sup>[1]</sup>.

Diabetic retinopathy (DR) is the most common microvascular complication of diabetes, and it remains one of the leading causes of blindness worldwide. During the first two decades of disease, nearly all patients with type 1 diabetes and over 60% of patients with type 2 diabetes develop DR<sup>[2]</sup>.

In diabetic retinopathy, chronic longstanding hyperglycemia results in dysfunction and death of endothelial cells, pericytes and vascular smooth muscle cells resulting in breakdown of the blood-retinal barrier and retinal ischemia from capillary non-perfusion<sup>[3]</sup>.

Although intravitreal drug therapy and laser photocoagulation are used to treat retinal neovascularization or macular edema that can occur as visually significant

complications of these common retinal vascular disorders, no treatment is available for vision loss resulting from retinal ischemia and/or retinal degeneration associated with these retinal vascular disorders<sup>[4]</sup>. Stem cell-based therapies have the potential effectivity in many human diseases including retinal disorders, and they have been proven to be safe and effective in a wide range of immunomediated diseases<sup>[5]</sup>.

Adipose derived mesenchymal stem cells (ADMSCs) are easily accessible in abundant quantities and can be collected by a minimally invasive procedure. Adipose tissue-derived stem cells showed properties similar to those of bone marrow-derived mesenchymal stem cells) MSCs (and showed even better isolation reproducibility and higher proliferation capacity<sup>[6-7]</sup>. Moreover, ASCs demonstrated four properties that could be helpful in cell therapy: angiogenicity, osteogenicity, immunomodulation and promotion of tissue remodeling<sup>[8]</sup>.

Therefore, this study was designed to clarify the histological changes that may occur in the retina of adult

male albino rats after induction of diabetic retinopathy, and to investigate the preventive effectiveness of ADMSCs in the treatment of retinal degeneration.

## MATERIAL AND METHODS

### Animals:

Forty adult healthy male Wistar albino rats (14-18 weeks) weighing 180 - 200 grams each, were used in this study. They were obtained from the breeding animal house, Faculty of Medicine, Zagazig University. The experimental protocol was approved by the Zagazig University Research Ethics Committee. The rats were kept in the animal house for one week in stainless steel cages to be acclimatized to the new environment before the experiment. They were maintained in accordance with the guidelines of stem cell research unit in the central laboratory, Zagazig University. Throughout the duration of the experiment, the rats were housed at room temperature with normal light/dark cycles. They were allowed ad-libitum access to food and water.

### Drugs and chemicals

- Streptozotocin (STZ) was obtained in the form of vials; each vial contains 1gm streptozotocin, manufactured by EIMC United Pharmaceuticals (EUP) Badr City, Cairo, Egypt.

- Adipose-derived mesenchymal stem cells (ADMSCs) labelled with Paul Karl Horan 26 (PKH-26) (red fluorescence cell linker) were provided from Biochemistry Department, Kasr Al-Ainy Medical School

Preparation of adipose derived-mesenchymal stem cells (ADMSCs): Human adipose tissue was obtained from patients undergoing tumescent liposuction. The adipose tissue was washed with Hank's Balanced Salt Solution (HBSS) (approximately 3 ml/g), re-suspended in 0.075% type IA collagenase (Sigma)/HBSS (approximately 2 ml/g), and incubated at 37°C for 1 h. The digested adipose tissue was passed through a 100- $\mu$ m filter to remove debris and centrifuged at 160  $\times$  g for 10 min to obtain a cell pellet. The pellet was re-suspended and washed twice with HBSS. After isolation, 30 ml of re-suspended cells were plated in expansion medium at a density of 5 $\times$ 10<sup>6</sup> nucleated cells/100 mm tissue culture dish and incubated at 37°C in a humidified environment containing 5% CO<sub>2</sub>. The expansion medium contained 58% DF-12 medium (Dulbecco's modified Eagle's medium/Ham's F-12 medium, Gibco), 40% MCDB (medium complete with trace elements-201, Sigma), 2% FCS (Gibco), 1 $\times$  insulin transferrin-selenium (ITS, Gibco), 1 $\times$ 10<sup>-9</sup>mol/l dexamethasone (Sigma), 1 $\times$ 10<sup>-4</sup>mol/l ascorbic acid 2-phosphate (Sigma), 20 ng/ml interleukin-6, 10 ng/ml epidermal growth factor (EGF), 10 ng/ml platelet derived growth factor (PDGF)-BB (Sigma), 100 U/ml penicillin, and 100  $\mu$ g/ml streptomycin (Gibco)<sup>[9]</sup>. Labeling of stem cells with Paul Karl Horan 26 (PKH-26) (red fluorescence cell linker): ADMSCs were harvested and labeled with PKH26 dye<sup>[10]</sup>. Cells were centrifuged and washed twice in serum free medium. They were pelleted and suspended in dye solution. Retinal tissue

was examined with a fluorescent microscope (Olympus BX50F4, No. 7M03285, Tokyo, Japan) to detect and trace the cells stained with PKH26 (Fig. 1).

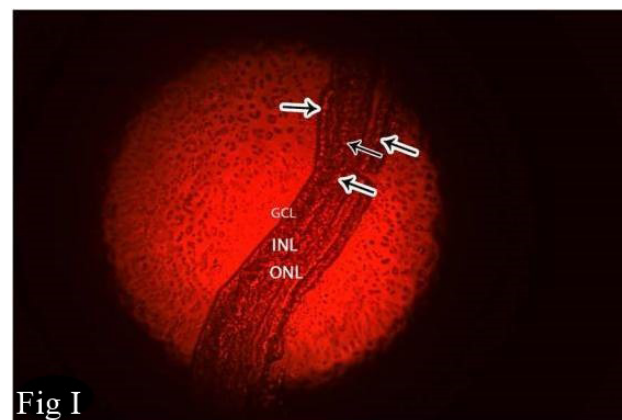


**Fig 1** : A photomicrograph of a section in Retinal tissue was examined with a fluorescent microscope (Olympus BX50F4, No. 7M03285, Tokyo, Japan) to detect and trace the cells stained with PKH26

(Immunoperoxidase reaction x 1000).

### Experimental procedure

After one week of acclimatization, the animals were divided into three groups:

- Group I (Control group): Included 20 rats that were equally subdivided into two subgroups:

- Subgroup IA (Negative control group): The rats of this group received no treatment.
- Subgroup IB: The rats were injected intravenously through the caudal vein with 0.5 ml ADMSCs (1 $\times$ 10<sup>7</sup> cells/ml) dissolved in phosphate buffered saline<sup>[11]</sup>.

- Group II (Diabetic group): Included 10 rats that were rendered diabetic with a single intraperitoneal injection of STZ (50 mg/kg) freshly dissolved in 0.9% saline solution<sup>[12]</sup>. Two days after STZ injection, the levels of blood glucose were measured with an Accu-check Sensor analyzer (Roche, Mannheim, Germany) and diabetes mellitus was confirmed. Rats with glucose levels 250 mg/dl or more were considered diabetic and used in the study. Blood glucose was monitored throughout the study to ensure that hyperglycemia was maintained and to treat any extreme glycemic levels with insulin. Retinal specimens were taken 4 weeks after establishment of DM<sup>[13]</sup>.

- Group III (Therapy group): Included 10 rats that were injected with STZ in the same previous regimen then the diabetic rats were injected intravenously through the caudal vein with 0.5 ml ADMSCs (1 $\times$ 10<sup>7</sup> cells/ml) suspended in phosphate-buffered saline<sup>[11]</sup>. Then, the specimens from rat  $\square$  retinae were taken four weeks after stem cell administration.

At the end of experiment, rats were anaesthetized with 200 mg/kg sodium pentobarbital solution intraperitoneally<sup>[14]</sup>, then both eyes were enucleated

and processed for histological examination; one for light microscope examination and the other for electron microscope examination. Samples from the retina were fixed in 10% neutral buffered formalin and processed for preparation of 5  $\mu\text{m}$  thick sections for histological examination; hematoxylin and eosin<sup>[15]</sup>, toluidine blue for semithin sections<sup>[16,17]</sup> and immunohistochemical analysis for caspase-3<sup>[18]</sup>. For ultrastructural study, specimens were immediately fixed in 2.5% phosphate-buffered glutaraldehyde (pH 7.4), postfixed in 1% osmium tetroxide in the same buffer at 4°C, dehydrated, and embedded in epoxy resin<sup>[15]</sup>.

## Methods:

### 1- Light microscopic study:

- Paraffin sections (5  $\mu\text{m}$  thick) stained with (HandE) for examination of overall morphology.
- Immunohistochemical study

Immunohistochemical reactions were carried out using the avidin-biotin peroxidase complex (Dako company, Wiesentheid/Bavaria, Germany, Biotin Blocking System, Code X0590) method following the manufacturer's instructions serial sections (4 $\mu\text{m}$ ) of paraffin-embedded specimens were deparaffinized on charged slides. The sections were incubated in 0.1% hydrogen peroxide for 10 min to block the endogenous peroxidase activity and then incubated with the primary antibody. The primary antibody used for caspase-3 was ready-to-use rabbit polyclonal antibody (CAT-No. RB-3425-R2). The slides were incubated with the secondary anti-rabbit antibody versal kits (Zymed laboratories), diluted 1:200 for 30 minutes, staining was completed by incubation with chromogen, called diaminobenzidine (DAB). Mayer's hematoxylin was used as a counterstain<sup>[18]</sup>.

### 2- Electron microscopic study:

Semithin sections (1 $\mu\text{m}$  thick) were stained with 1% toluidine blue for light microscopic examination. Ultrathin sections were stained with uranyl acetate and lead citrate<sup>[15]</sup>. The prepared sections were examined and photographed by JOEL EM 1010 transmission electron microscope at Electron Microscope Research Laboratory (EMRL), Histology and Cell Biology Department, Faculty of Medicine, EL Azhar University. The negative films were developed and printed. In both procedures, developer and fixer were needed.

### 3- Morphometric study:

The image analyzer computer system Leica Qwin 500 (Leica Ltd, Cambridge, UK) in the image analyzing unit of the Pathology Department, Faculty of Dentistry, Cairo University, Cairo, Egypt, was used to evaluate the thickness of INL and the area percentage (area %) of positive immunoreaction for caspase-3. It was measured from x 400 photomicrographs using Digimizer 4.3.2. image analysis software (MedCalc Software bvba, Belgium). The area

percentage of caspase-3 immunostaining was measured by using the NIH Image J (v1.50) program.

### 4- Statistical analysis:

Statistical analysis was measured for the thickness of INL and the area percentage of caspase-3 immunostaining. Data for all groups were expressed as mean  $\pm$  SD ( $X \pm SD$ ). The data obtained from the image analyzer and the biochemical data were subjected to SPSS program version 14 (Chicago, Illinois, USA). Statistical analysis using the one-way analysis of variance test was carried out. The results were considered statistically significant as *P* value was less than 0.05<sup>[19]</sup>.

## RESULTS

### Histological Results:

#### Group I (Control group):

##### A - Light microscope examination:

Examination of hematoxylin and eosin-stained sections of the retina of the control rats showed photoreceptor layer (PL), outer nuclear layer (ONL) which contained deeply stained nuclei of rods and cones, outer plexiform layer (OPL) that appeared as a narrow pale zone, and inner nuclear layer (INL). Inner plexiform layer (IPL) appeared as pale zone between INL and ganglion cell layer (GCL). Nerve fiber layer (NFL) was also seen. Fibers of Muller cells were detected in OPL, GCL and NFL (Fig. 1).

Toluidine blue-stained semi-thin sections of the control retina revealed different layers that were arranged as following: retinal pigment epithelium layer (RPE), photoreceptor layer (PL) that contained the photoreceptor processes, and ONL which was formed of closely-packed, deeply stained nuclei of rods and cones arranged in rows. The outer plexiform layer (OPL) appeared as a pale-stained loose reticular zone that contained blood capillaries. Inner to the OPL, there was the INL occupied by cell bodies of different neurons, mostly bipolar ones. Muller cells with their irregular shape and deeply stained nuclei were observed. Amacrine and horizontal cells were also seen. Nuclei in the INL appeared larger and paler than those in the ONL. Inner plexiform layer (IPL) appeared as a pale stained area. Ganglion cell layer (GCL) contained large ganglion neurons with lightly stained cytoplasm and vesicular nuclei. Finally, the inner limiting membrane was observed (Fig. 2 A, B and C).

Immunohistochemically, sections of the control retina showed negative reaction for caspase-3 in cells of all retinal layers (Fig. 3).

##### B- Electron microscope examination:

Ultrastructurally, sections in the retina of the control rats showed RPE composed of cuboidal cells with oval nuclei, resting on Bruch's membrane. Numerous invaginations of the basal membranes associated with mitochondria were observed (Fig. 4).

The outer segments of photoreceptor cells (POS) appeared as elongated, straight, cylindrical structures. They contained flattened, horizontal, lamellar discs formed by infoldings of their plasma membrane. Each disc was composed of a bi-membranous layer enclosing a space in between (Fig. 5). The inner segments of photoreceptor cells (PIS) were long and condensed and contained elongated mitochondria with intact cristae. The outer limiting membrane was observed as an electron-dense line separating the PIS from the ONL (Fig. 6 A and B). The outer nuclear layer (ONL) was occupied by nuclei of rods and cones with minimal intercellular spaces. Rod nuclei were heterochromatic and surrounded by a thin rim of cytoplasm. However, cone nuclei were less heterochromatic (Fig. 7). The OPL appeared with ovoid transverse sections in the terminal synaptic process of the photoreceptors, containing round mitochondria (Fig. 8). The inner nuclear layer contained the nuclei of bipolar and Muller cells. Bipolar cells contained euchromatic nuclei with peripheral heterochromatin condensation. Muller glial cells were irregular in shape with euchromatic nuclei, RER, mitochondria and cytoplasmic processes (Fig. 9 A and B). The ganglion cell layer contained cell bodies of large multipolar neurons; ganglion cells, with oval euchromatic nuclei, mitochondria and RER. The optic nerve fiber layer contained un-myelinated axons of the ganglion cells. The inner limiting membrane was also observed (Fig. 10).

### **Group II (Diabetic group):**

#### **A - Light microscope examination:**

Hematoxylin and eosin-stained sections in the retina of the diabetic rats showed disruption in the retinal architecture. The photoreceptor layer (PL) revealed loss of some photoreceptor processes, and vacuolation. There were marked thinning of OPL, loss of cells in ONL and INL, and thinning of INL with small dark nuclei. Also, the IPL showed wide spaces between nerve fibers, and few ganglion cells were seen with small dark nuclei (Fig. 11 A and B).

Semi-thin sections showed widely separated nuclei in both ONL and INL indicating loss of cells (Fig. 12).

Immunohistochemically, there was strong cytoplasmic reaction for caspase-3 in ONL, INL, IPL and GCL (Fig. 13).

#### **B- Electron microscope examination:**

Ultrastructurally, retinal specimens of the diabetic retina showed the RPE with poorly-developed basal infoldings and dense bodies. Its cytoplasmic processes projected between the outer segments of photoreceptors (Fig. 14). Distortion and focal destruction of lamellar discs of the outer segments of photoreceptors were seen (Fig. 15). There were wide spaces between photoreceptor nuclei in ONL. Un-myelinated axons and vacuoles were seen in OPL (Fig. 16). Many deeply-stained Muller cells with their processes were seen in the INL. Bipolar cells contained mitochondria with distorted cristae (Fig. 17). Ganglion cells showed irregular dark nuclei and vacuolated cytoplasm (Fig. 18).

### **Group III (Therapy group): 4 weeks after stem cell administration:-**

#### **A - Light microscope examination:-**

Using fluorescent microscope, examination of sections from the retina, four weeks after stem cell administration, showed distribution of PKH26-labeled cells as bright dots within ONL, INL and GCL (Fig. 19).

Hematoxylin and eosin stained-sections of the retina showed improvement of the retinal architecture. There were few spaces between cells in ONL and INL. Ganglion cells were seen with their pale vesicular nuclei (Fig. 20).

Semi-thin sections showed improvement of the retinal architecture including RPE, outer and inner segments of photoreceptors, ONL, INL, IPL and GCL (Fig. 21 A and B).

Immunohistochemically, there was negative reaction for caspase - 3 in cells of all retinal layers (Fig. 22).

#### **B- Electron microscope examination:-**

Ultrastructurally, the retina of ADMSCs-treated group showed structure nearly similar to the control. There were improved photoreceptor processes with intact lamellar bodies, and narrow spaces between photoreceptor nuclei (Figs. 23 and 24). The inner nuclear layer showed many deeply stained Muller cells with their processes, and bipolar cells (Fig. 25). There were ganglion cells with indented nuclei in GCL (Fig. 26).

### **Morphometric and Statistical Results:**

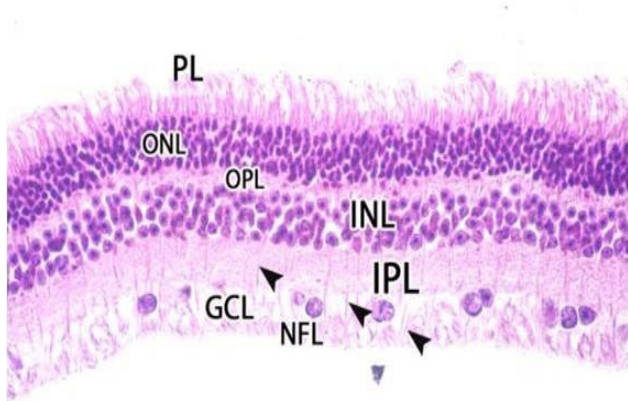
Our results revealed no significant difference between subgroups IA and IB. Therefore, the average of group I was used as a control to be compared with the other groups.

#### **1) Thickness of INL:**

Statistical analysis of the thickness of INL ( $\mu\text{m}$ ) by one-way ANOVA test revealed highly significant difference between the different studied groups as the  $p$  value  $< 0.005$ . LSD for comparison between groups revealed highly significant decrease in the thickness of INL in group II (diabetic group) as compared to group I (control group) and group III (therapy group). However, there was no statistically significant difference between group III and group I (Tables 1 A, 1 B).

#### **2) The area percentage of immunoreaction for caspase-3:**

Statistical analysis of the area percent of immune reaction for caspase-3 by one-way ANOVA test revealed highly significant difference between the different studied groups as the  $p$  value  $< 0.005$ . LSD for comparison between groups revealed highly significant increase in area percent for caspase-3 in group II as compared to both group I and group III. However, there was no statistically significant difference between group III and group I (Tables 2 A, 2 B).



1

**Fig.1:** A photomicrograph of a section in a control adult rat's retina showing photoreceptor layer (PL), outer nuclear layer (ONL), outer plexiform layer (OPL), inner nuclear layer (INL), inner plexiform layer (IPL), ganglion cell layer (GCL) and nerve fiber layer (NFL). Fibers of Muller cells (arrow head) are seen in IPL, GCL and NFL. (HandE x 400).

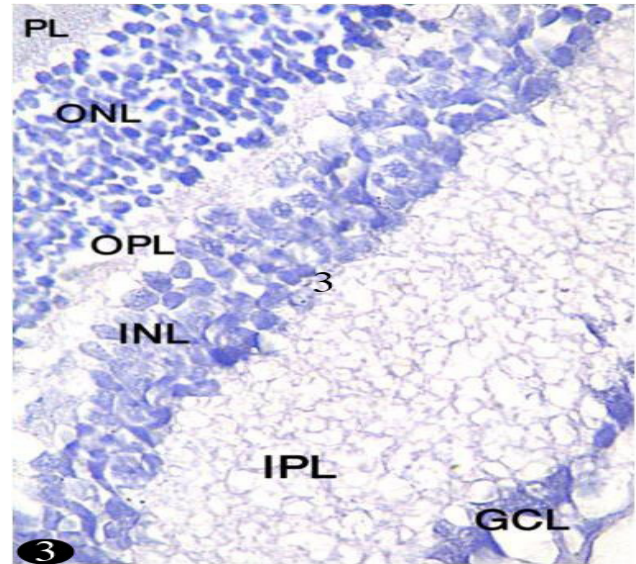


**Fig.3:** A photomicrograph of a section in a control adult rat's retina showing negative reaction for caspase-3 in cells of all retinal layers. (Immunoperoxidase reaction x 1000).

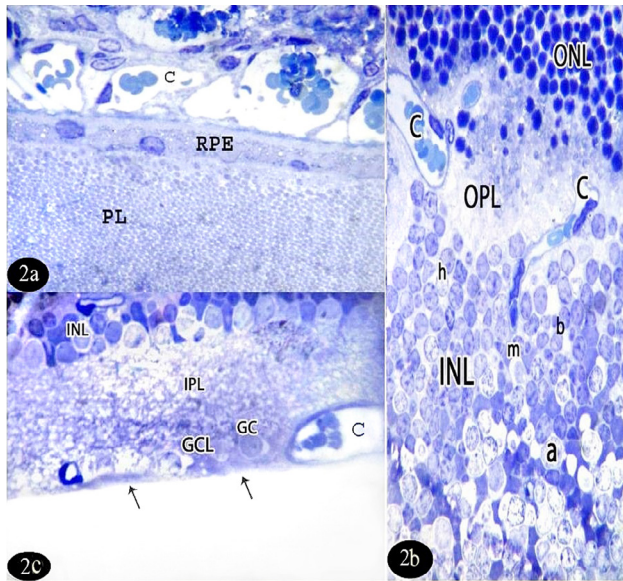


**Fig.2:** A photomicrograph of a semi-thin section in a control adult rat's retina showing: (a): retinal pigment epithelial cells (RPE), blood capillary (C) and photoreceptor layer (PL). (b): Dark nuclei of rods and cones in ONL. The OPL appears as loose reticular layer containing blood capillaries (C). Nuclei in INL are larger and paler than those in ONL. Different types of cells are recognized; bipolar (b), Muller (M), amacrine (a) and horizontal (h) cells. (c): GCL reveals a single row of ganglion cells (GC) with lightly stained cytoplasm and vesicular nuclei. Notice, blood capillaries (C). (Toluidine blue x1000).

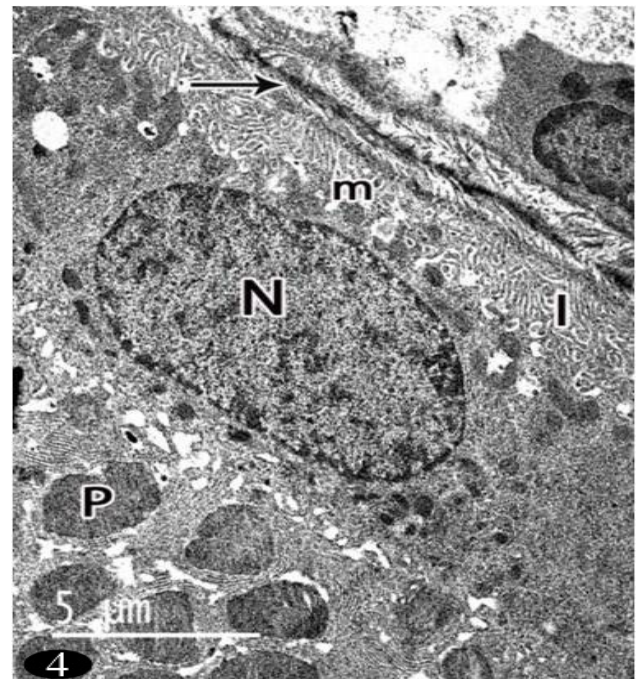


**Fig.4:** A photomicrograph of a section in a control adult rat's retina showing a pigment epithelial cell with oval nucleus (N), resting on Bruch's membrane (arrow). Numerous invaginations of the basal membrane (I) associated with mitochondria (m) are observed. Processes of rods and cones (P) are also seen. (TEM x7000).

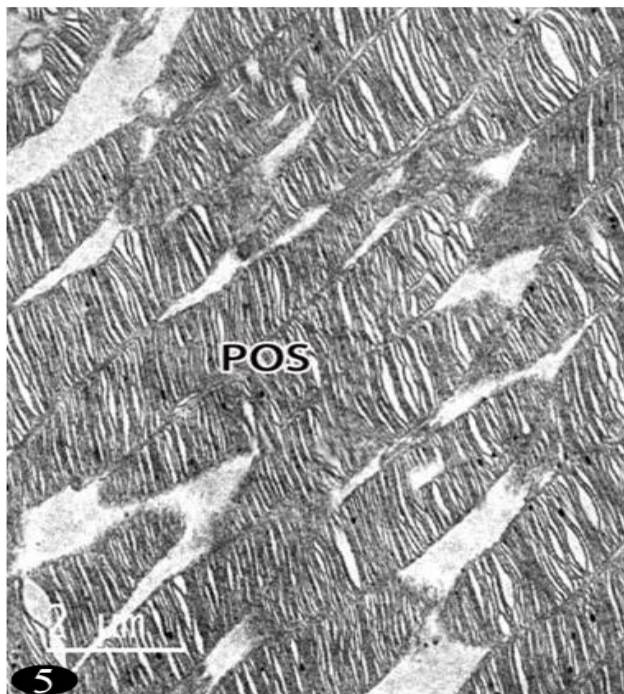


**Fig. 5:** A photomicrograph of a section in a control adult rat's retina showing the outer segments of rods photoreceptors (POS) as elongated, straight, cylindrical structures containing flattened horizontal lamellar discs. (TEM x 11500).

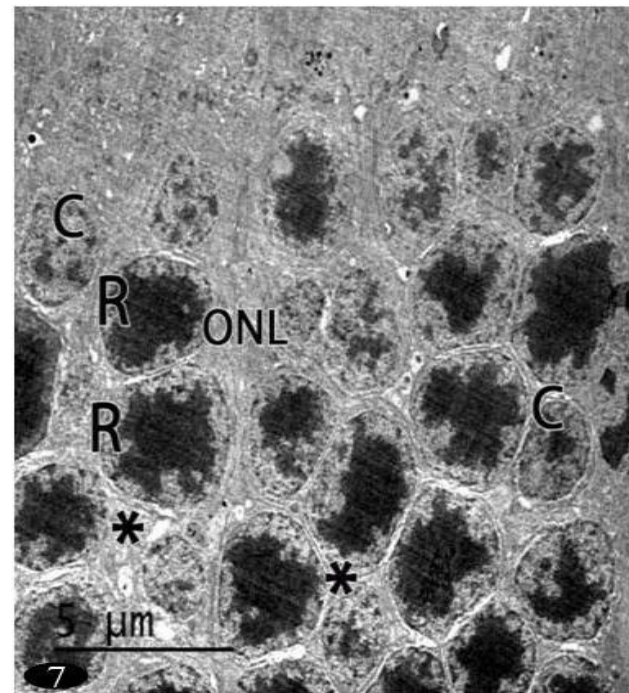


**Fig. 7:** A photomicrograph of a section in a control adult rat's retina showing the ONL formed of rods (R) and cones (C) cell bodies with minimal intercellular spaces (\*). Rod nuclei are characterized by heterochromatin condensation, and surrounded by a thin rim of cytoplasm. However, cone nuclei are less heterochromatic. (TEM x 6000).

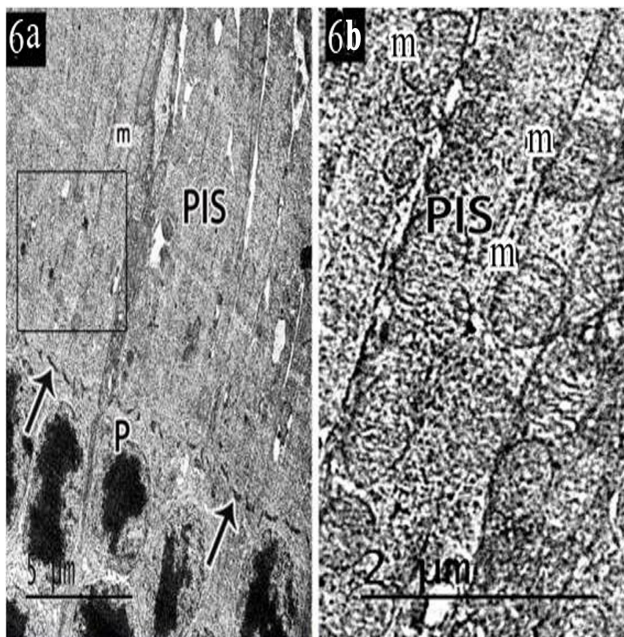


**Fig. 6:** A photomicrograph of a section in a control adult rat's retina showing: (a): inner segments of photoreceptor cells (PIS) containing elongated mitochondria (m). The outer limiting membrane is observed as an electron dense line (arrow). The ONL shows cell bodies of photoreceptors (P) with characteristic dense chromatin and minimal intercellular spaces (TEM x 7200). (b): higher magnification of a boxed area of Fig. 6a showing the photoreceptor cell inner segments (PIS) containing mitochondria (m) with intact cristae. (TEM x 18000).

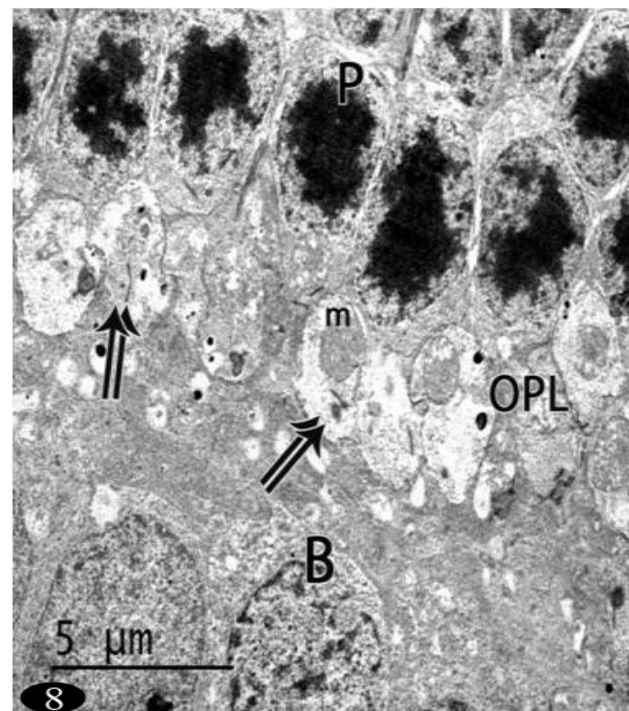


**Fig. 8:** A photomicrograph of a section in a control adult rat's retina showing OPL with ovoid transverse sections in the terminal synaptic process of the photoreceptors (double arrows) containing mitochondria (m). The nuclei of photoreceptors (P) and bipolar cells (B) are also observed. (TEM x 6000).

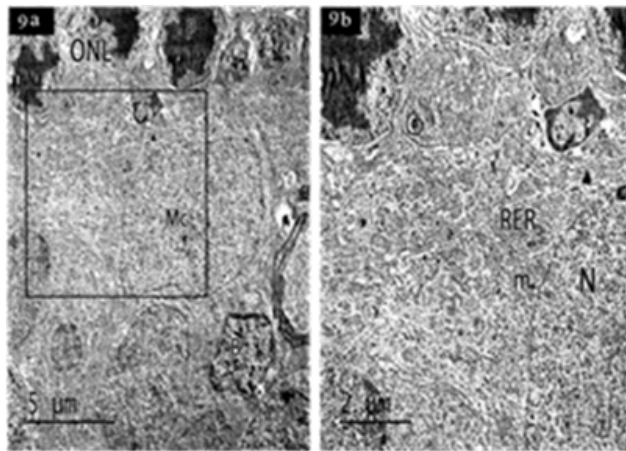
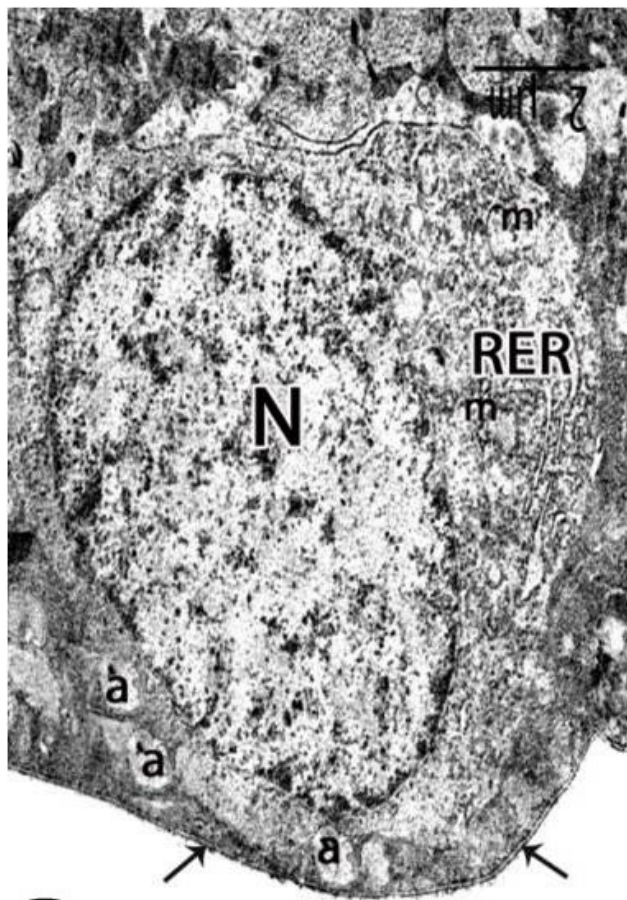


**Fig.9:** A photomicrograph of a section in a control adult rat's retina showing: (a): Muller cell (Mc) which appears irregular in shape with euchromatic nucleus. Bipolar neurons (B) containing euchromatic nuclei with peripheral heterochromatin are also seen. (b): Higher magnification of the boxed area showing part of Muller cell with euchromatic nucleus (N), rough endoplasmic reticulum (RER) and mitochondria (m). (TEM a, x 6000 and b, x 12000).



**10**  
**Fig. 10:** A photomicrograph of a section in a control adult rat's retina showing a ganglion neuron with oval euchromatic nucleus (N), mitochondria (m), and (RER). The unmyelinated axons (a) in the nerve fiber layer and the inner limiting membrane (arrow) are seen. (TEM x 9500).

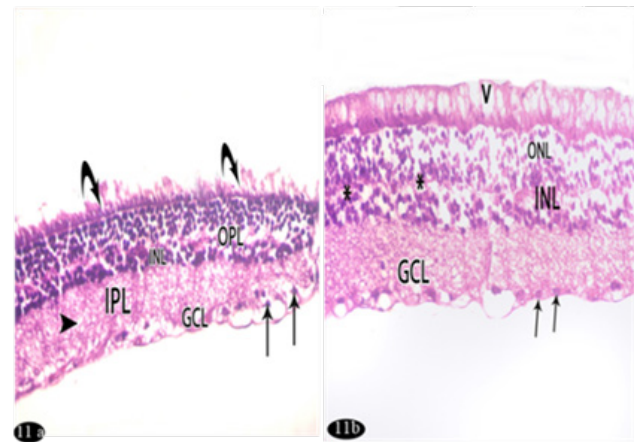
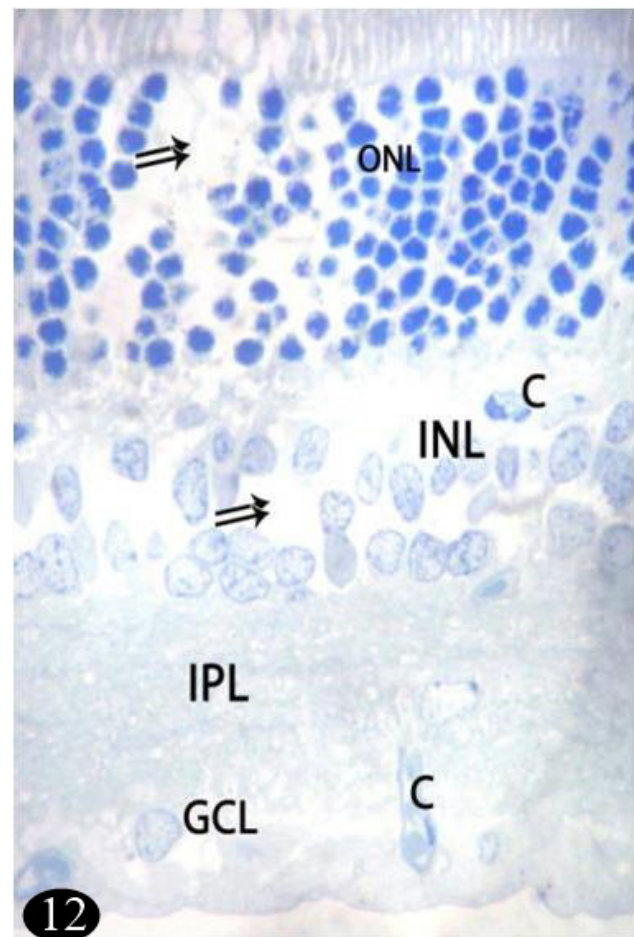


**Fig. 11:** A photomicrograph of a section in a diabetic rat's retina showing disruption of the normal architecture. (a): Some photoreceptor processes are lost (curved arrow). The outer plexiform layer (OPL) appears thin. There is also marked thinning in the INL with pyknotic nuclei. Widening of spaces between nerve fibers in the IPL is also observed (arrow head). In GCL, cells have small dark nuclei (arrow). (b): Vacuoles in photoreceptor layer (V), loss of cells in ONL and INL and marked thinning of OPL (\*). (H and E x 400).



**12**  
**Fig.12:** A photomicrograph of a semi-thin section in a diabetic rat's retina showing widely separated nuclei (double arrows) in both ONL and INL. Notice, Blood capillaries (C). (Toluidine blue x1000).

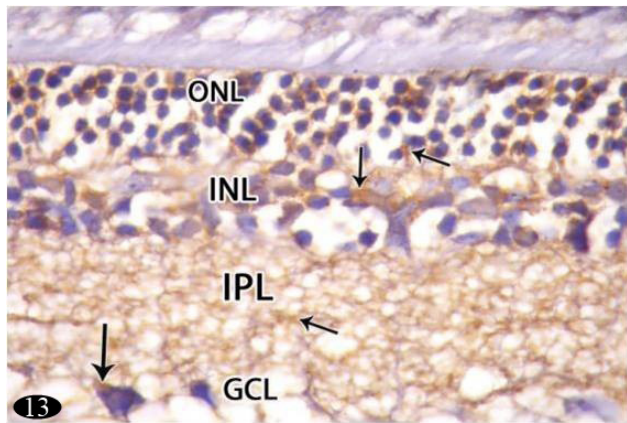


**Fig.13:** A photomicrograph of a section in a diabetic rat's retina showing strong cytoplasmic reaction for caspase-3 (arrow) in ONL, INL, IPL and GCL. (Immunoperoxidase reaction x 1000).

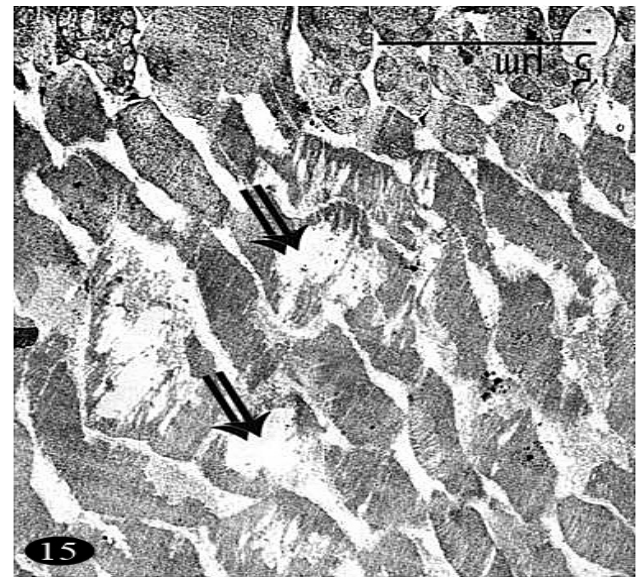


**Fig.15:** A photomicrograph of a section in a diabetic rat's retina showing outer segments of photoreceptors with distorted lamellar discs (double arrows). (TEM X 7200).

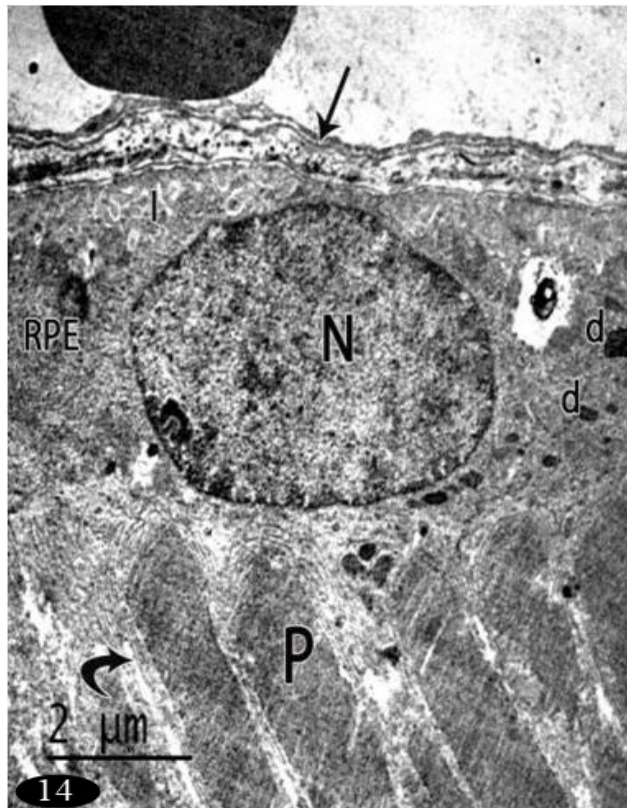


**Fig. 14:** A photomicrograph of a section in a diabetic rat's retina showing RPE with poorly developed basal infoldings (I) and dense bodies (d). Its cytoplasmic processes (curved arrow) project between outer segments of photoreceptors (P). Notice, euchromatic nucleus (N) and Bruch's membrane (arrow). (TEM X 12000).

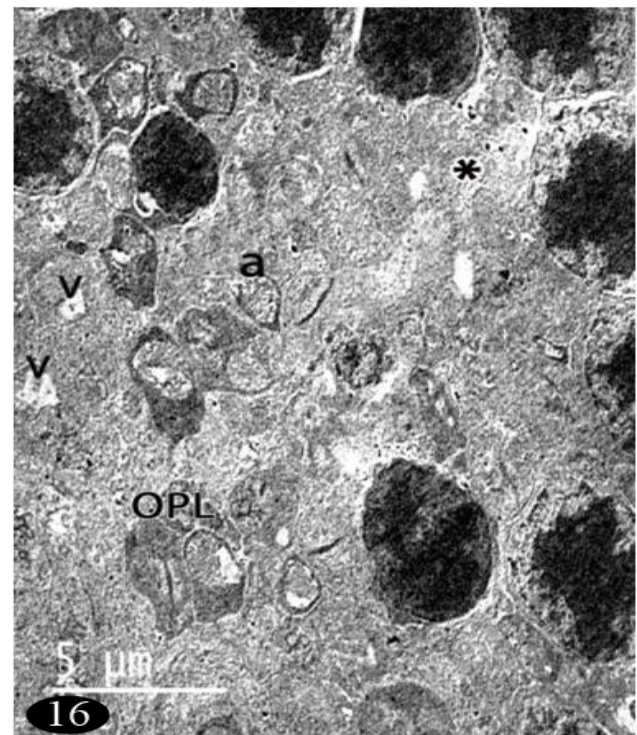


**Fig. 16:** A photomicrograph of a section in a diabetic rat's retina showing wide spaces between photoreceptor nuclei (\*). Vacuoles (v) and unmyelinated axons (a) are seen in OPL. (TEM X 5800).

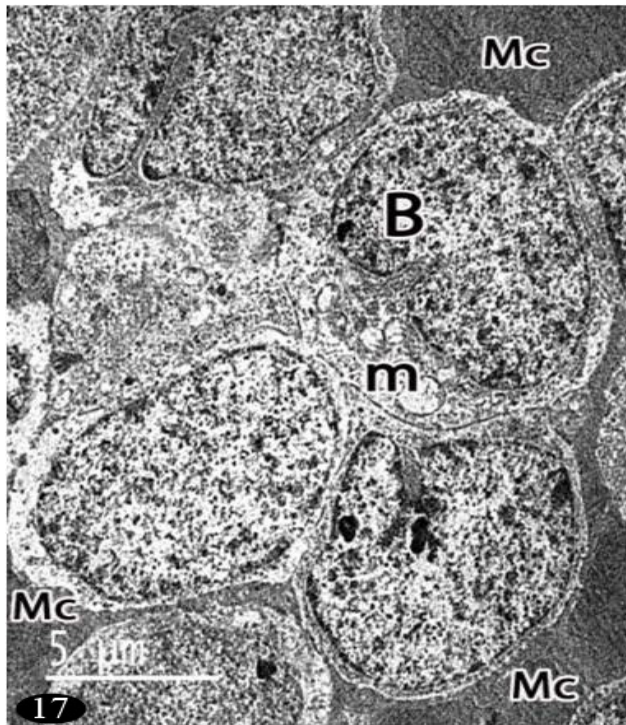


**Fig. 17:** A photomicrograph of a section in a diabetic rat's retina showing a bipolar cell (B) containing mitochondria with distorted cristae (m). Muller cells (Mc) are seen with their processes. (TEM X 5800).

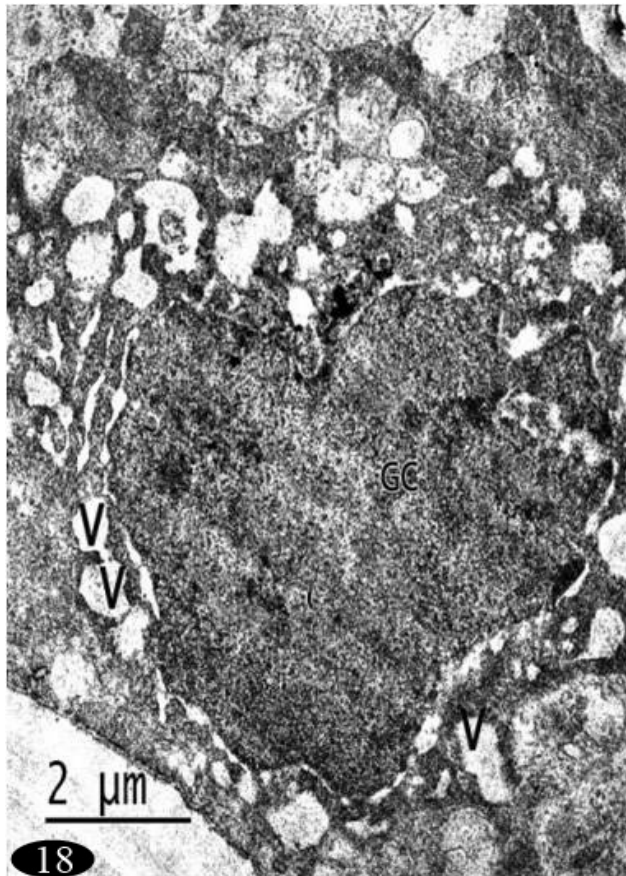


**Fig. 18:** A photomicrograph of a section in a diabetic rat's retina showing a ganglion cell (GC) with irregular nucleus and cytoplasmic vacuoles (v). (TEM X 12000).

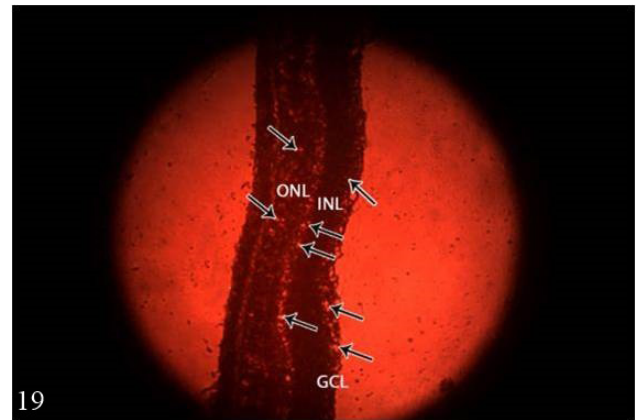


**Fig. 19:** A photomicrograph of a section in rat's retina, four weeks after stem cell administration showing distribution of PKH26-labeled cells (arrow) appearing as bright dots within ONL, INL and GCL. (Fluorescent Microscope x 200).

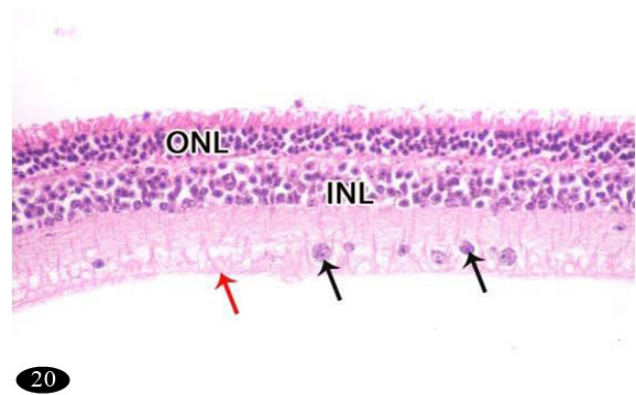


**Fig. 20:** A photomicrograph of a section in rat's retina, four weeks after stem cell administration showing structure nearly similar to the control group. There are few spaces between cells in the ONL and INL. Ganglion cells are seen with their euchromatic nuclei (black arrows). Notice, ILM (red arrow). (HandE x 400)

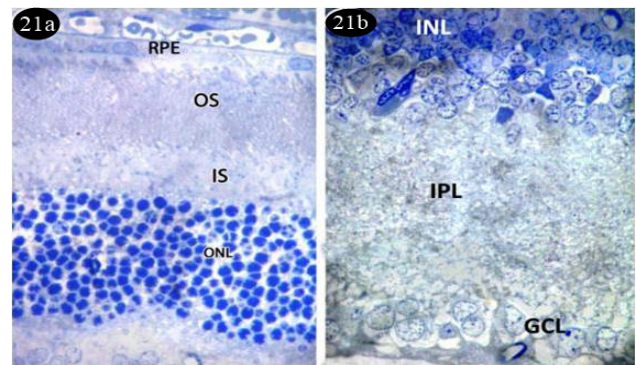


**Fig. 21:** A photomicrograph of a semi-thin section in rat's retina, four weeks after stem cell administration showing retinal architecture nearly similar to the control. In (a): retinal pigment epithelial cells (RPE), outer (OS) and inner (IS) segments of photoreceptors, and ONL with dark nuclei and minimal intercellular spaces are seen. In (b): INL with larger and paler nuclei and minimal intercellular spaces, IPL and GCL with their pale cytoplasm are seen. (Toluidine blue x1000).

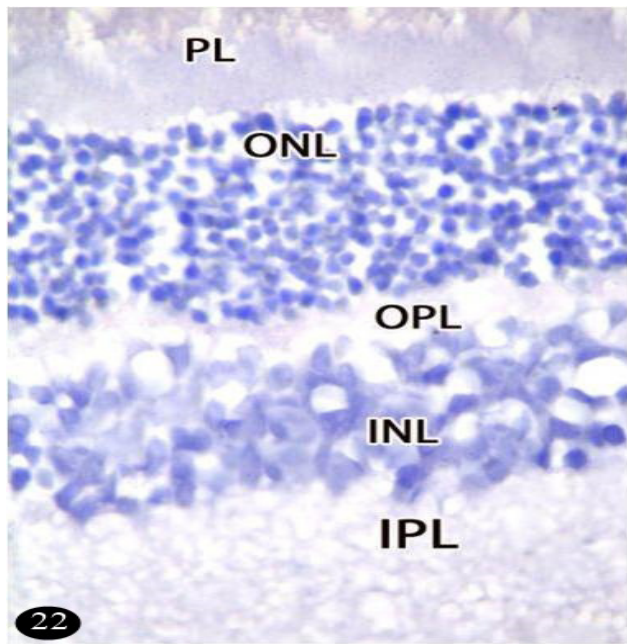


**Fig. 22:** A photomicrograph of a section in rat's retina, four weeks after stem cell administration showing negative reaction for caspase-3 in cells of all retinal layers. (Immunoperoxidase reaction x 1000)

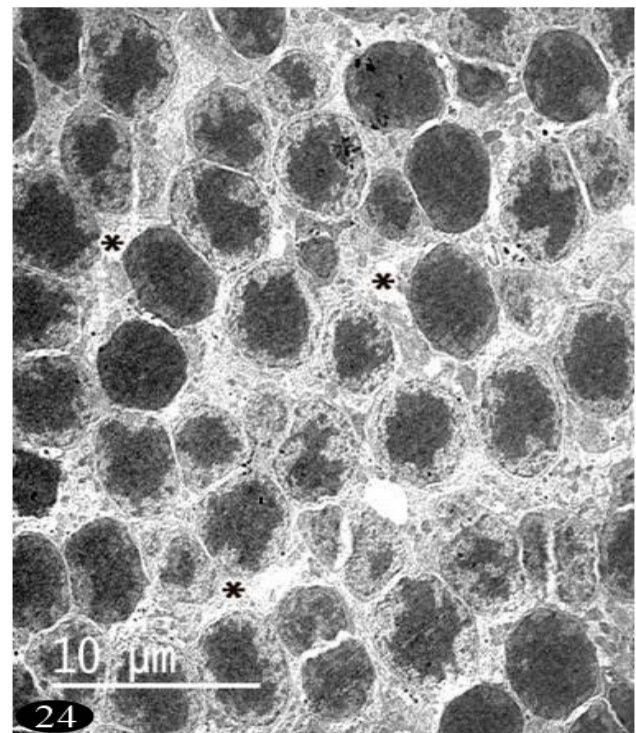


**Fig. 24:** A photomicrograph of a section in rat's retina, four weeks after stem cell administration showing narrow spaces between photoreceptor nuclei (\*). (TEM X 3400).



**Fig. 23:** A photomicrograph of a section in rat's retina, four weeks after stem cell administration showing improved outer segments of photoreceptor processes (OS) with intact lamellar bodies. (TEM X 18400).

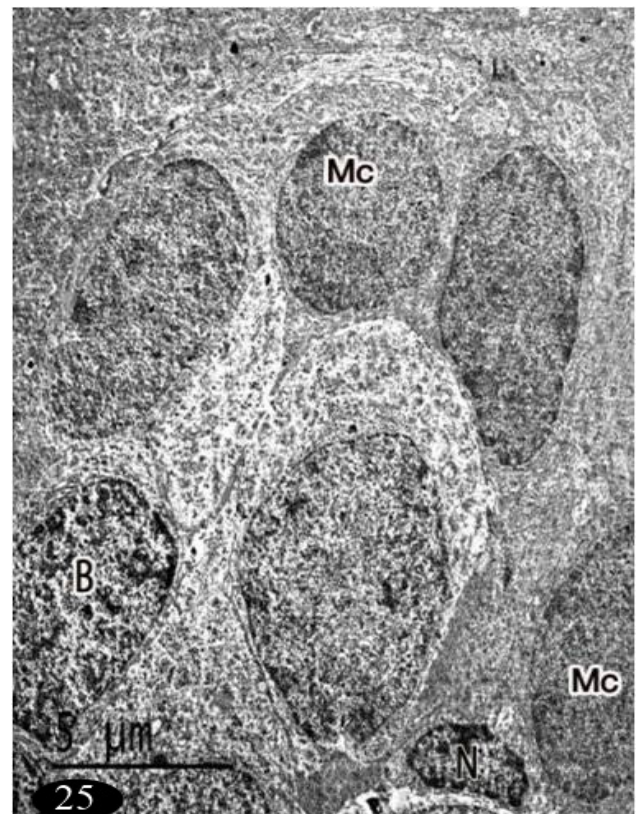


**Fig. 25:** A photomicrograph of a section in rat's retina, four weeks after stem cell administration showing many deeply stained Muller cells (Mc) with their processes, and bipolar cells (B). Notice, a cell containing small nucleus (N) with heterochromatin condensation. (TEM X 6000).

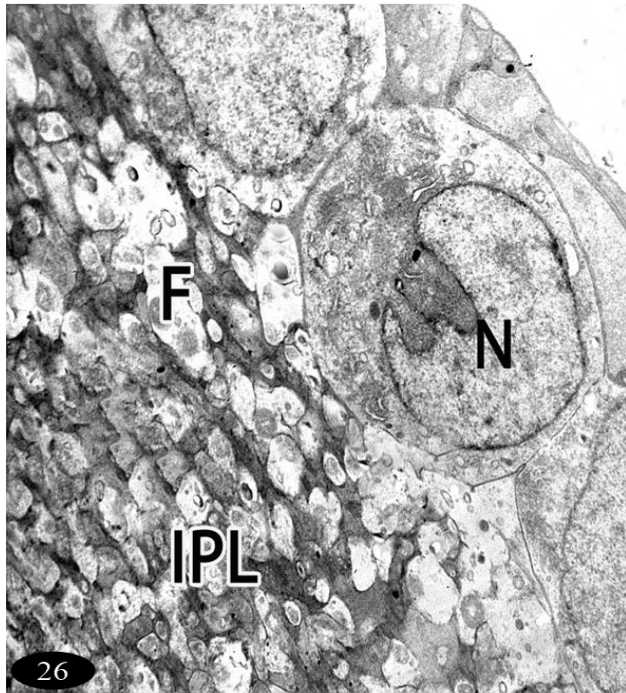


**Fig. 26:** A photomicrograph of a section in rat's retina, four weeks after stem cell administration showing ganglion cells with euchromatic nuclei (N). Notice nerve fibers (F) in the IPL. (TEM X 6000).

## DISCUSSION

In the current study, of ADMSCs were intravenously administered due to the risk of possible endophthalmitis, retinal detachment and hemorrhage associated with repeated intravitreal injections. In addition, the inner limiting membrane may limit the distribution of stem cells in the retina<sup>[20]</sup>.

Ultrastructurally, the retina of STZ-treated group showed poorly developed basal infoldings of RPE cells. In contrast, other researchers found no change in RPE in diabetic Long-Evans Tokushima Fatty Rats<sup>[21-22]</sup>. Also, the retina of diabetic group showed distorted lamellar discs of photoreceptor outer segments. Previous studies reported outer segment disorganization. On the contrary, other authors found that diabetes cause only reduction in the length of rod outer segments<sup>[22-23]</sup>.

The retinae of STZ-treated group showed loss of cellular elements in the outer nuclear layer with widely separated nuclei and presence of vacuoles. These vacuoles were attributed to neurodegeneration in the outer retina as a result of hyperglycemia<sup>[24]</sup>. An evidence of occurrence of apoptosis of few photoreceptors at 4 weeks of diabetes, and increase in their number afterwards was provided<sup>[22]</sup>. On the other hand, no difference was recorded in the thickness of photoreceptor layer between diabetics and normal subjects<sup>[25]</sup>. These authors also reported that the outer retina was not significantly influenced by diabetes at least in the early stages of disease, whereas the inner retina was precociously affected. Kern and Berkowitz<sup>[26]</sup> attributed the photoreceptor loss was less to diabetes than to other differences (including strain differences), and also

to duration of diabetes which plays an important role in the process.

Our results also revealed marked thinning in the INL with small dark stained nuclei in the diabetic group which was confirmed statistically as there was a highly significant decrease in the thickness of INL in diabetic group as compared to the other groups. These results were attributed to apoptotic death of inner retinal neurons<sup>[27]</sup>. Also, neural apoptosis, loss of ganglion cell bodies, glial reactivity and reduction in the thickness of the inner retinal layers in early stages of DR were due to the decay of the neural components affected by the altered biochemical environment including the glucose transport system<sup>[28-29]</sup>.

In our work, cells with small dark nuclei were observed in GCL of STZ-treated group. It was reported that inflammation, oxidative stress or exposure to advanced glycation end products might contribute to retinal ganglion cells apoptosis<sup>[30, 6, 31]</sup>.

Our study provided an evidence for apoptosis in the retina of the diabetic rats as there was strong positive cytoplasmic reaction for caspase-3 in cells of ONL, INL, IPL, and GCL. These results were confirmed statistically as a highly significant increase in area percentage for caspase-3 was observed in the diabetic group as compared to the control. The expression of several pro-apoptosis molecules in retina from human diabetic eyes (caspase -3, Fas, and Bax) was proved<sup>[32]</sup>. Moreover, it was recorded that the number of active caspase-3-immunoreactive cells was increased in the ganglion cell layer and there was a cumulative loss of retinal ganglion cells and amacrine cells in diabetic mice<sup>[33]</sup>.

In our study, many deeply-stained Muller cells were observed the diabetic retina. In the same context, it was reported that Muller cells are particularly susceptible to hyperglycemia causing consequent hypertrophy of Muller cells in the earlier stages of DR<sup>[34-35]</sup>. Hyperglycemia was found to increase the release of reactive oxygen species (ROS) and the synthesis of diacylglycerol (DAG) increasing the activity of protein kinase C (PKC); a major pathway implicated in changes characteristic of diabetic retinopathy such as increased vascular permeability, neovascularization, endothelial proliferation and apoptosis<sup>[36, 37, 38]</sup>.

The metabolic and the morphological alterations of Muller cells encouraged secondary progressive neuronal loss, due to the crucial role of Muller cells in mediating relationship between retinal vessels and neurons<sup>[39]</sup>. Furthermore, the ability of Müller cells (the principal glia of the retina) in the conversion of glutamate released by neurons to glutamine was reduced. consequently, glutamate accumulates to excessive levels leading to uncontrolled influx of intracellular calcium ions causing neurotoxicity<sup>[40]</sup>.

In contrast with our study, Li and Puro<sup>[41]</sup> observed increased thickness of INL and OPL in diabetic

patients versus controls. They attributed this finding to the hyperplasia of Muller cells in DM which leads to increased number of nuclei that was demonstrated histopathologically. The number of cell nuclei in the INL reached a multiplication factor of 1.6 times, at 20 weeks of DM. It was also suggested that the increased retinal thickness and water content observed in diabetic rats was due to diffuse central edema<sup>[42]</sup>.

The increased concentrations of cytokines, particularly vascular endothelial growth factor (VEGFA), interleukin (IL)-1 $\beta$ , IL-6, IL-8, tumor necrosis factor (TNF)- $\alpha$ , and monocyte chemoattractant (MCP)-1 in the vitreous of patients with proliferative diabetic retinopathy and diabetic macular edema have a role in the pathology of several diabetic complication<sup>[43, 44]</sup>. Additionally, diabetes depletes the content of brain-derived neurotrophic factor (BDNF) in both brain and retina; the growth factor which was suggested to be particularly important for amacrine cell survival in the inner retina<sup>[45]</sup>.

The present work showed improvement in the retinal structure four weeks after ADMSCs administration. Immunohistochemically, negative reaction for caspase -3 was detected in cells of all retinal layers. These findings were confirmed statistically as there was no significant difference between group III and the control group. Great improvement in the retina of different experimental animals treated with ADMSCs was reported<sup>[46-47]</sup>. This improvement was referred to differentiation of ADMSCs cells into endothelial and neural cells with nestin expression and protection of photoreceptors in the diseased retina<sup>[48-49]</sup>. ADMSCs expressed insulin, glucagon, and somatostatin suggesting that may participate in the repair of damaged pancreatic tissue and lower blood glucose levels<sup>[50]</sup>.

Intravenous injection of ADMSCs in the STZ-induced DR rat model demonstrated an improvement in blood glucose levels and blood retinal barrier (BRB) integrity, with few donor cells differentiated into photoreceptor or astrocytes-like cells<sup>[20]</sup>. In addition, it was reported that the paracrine trophic factors released by ADMSCs play key roles by both stabilizing vasculature, and protecting retinal cells from diabetic damage<sup>[51-53]</sup>. In favor of this hypothesis, ADMSCs have been shown to secrete physiologically relevant levels of several anti-apoptotic, anti-inflammatory, and chemotactic proteins which have been shown to mediate some of the beneficial effects of MSC<sup>[53]</sup>.

## CONCLUSION

In our work, ADMSCs was proved to be effective in prevention of retinopathy in experimentally-induced diabetic model of adult male albino rats. This might represent a valuable tool for stem cell-based therapy in the future after clinical trials to adjust dose and ensure patient safety.

## CONFLICT OF INTEREST

There are no Conflicts of interest.

## REFERENCES

1. Magee MJ, Narayan KM. Global confluence of infectious and non-communicable diseases, the case of type 2 diabetes. *Preventive medicine* 2013; 57(3): 149–151.
2. Fong DS, Aiello L, Gardner TW, King GL, Blankenship G, Cavallerano JD, Ferris FL, Klein R. Retinopathy in diabetes. *Diabetes Care* 2004; 27(1): 84–87.
3. Kern TS, Tang J, Berkowitz BA. Validation of structural and functional lesions of diabetic retinopathy in mice. *Molecular vision* 2010; 16: 2121–2131.
4. Lois N, Carter RV, O'Neill C, Medin RJ, Stitt AW. Endothelial progenitor cells in diabetic retinopathy. *Frontiers in endocrinology* 2014; 5:1-11.
5. Zhang W, Wang Y, Kong J, Dong M, Duan H, and Chen S. Therapeutic efficacy of neural stem cells originating from umbilical cord-derived mesenchymal stem cells in diabetic retinopathy. *Sci Rep.* 2017; 7: 408.
6. Kern TS. Contributions of inflammatory processes to the development of the early stages of diabetic retinopathy. *Journal of Diabetes Research* 2007; 1-14.
7. Schubert T, Xhema D, V eriter S, Schubert M, Behets C, Delloye C. The enhanced performance of bone allografts using osteogenic-differentiated adipose-derived mesenchymal stem cells. *Biomaterials* 2011; 32(34): 8880–8891.
8. Lafosse A, Desmet C, Aouassar N, Andre W, Hanet MS, Beauloye C. Autologous adipose stromal cells seeded on a human collagen matrix for dermal regeneration in chronic wounds: clinical proof of concept. *Plastic and Reconstructive Surgery* 2015; 136(2): 279-295.
9. Cao Y, Sun Z, Liao L, Meng Y, Han Q, Zhao RC. Human adipose tissue-derived stem cells differentiate into endothelial cells in vitro and improve postnatal neovascularization in vivo. *Biochemical and biophysical research communications* 2005; 332(2): 370-379.
10. Haas SJ, Bauer P, Rolfs A, Wree A. Immunocytochemical characterization of in vitro PKH26-labelled and intracerebrally transplanted neonatal cells 2000; *Acta Histochemistry.* 102: 273-280.
11. Ezquer FE, Ezquer ME, Parrau DB, Carpio D, Yanez AJ, Conget PA. Systemic administration of multipotent mesenchymal stromal cells reverts hyperglycemia and prevents nephropathy in type 1 diabetic mice. *Biology Blood Marrow Transplantation* 2008; 14:631–640.

12. Abdollahi M, Zuki ABZ, Goh YM, Rezaeizadeh A, Noordin MM. Effects of Momordica charantia on pancreatic histopathological changes associated with streptozotocin-induced diabetes in neonatal rats. *Histology Histopathology* 2011; 26: 13-21.
13. Annadurai T, Muralidharan AR, Joseph T, Hsu MJ, Thomas PA, Geraldine P. Antihyperglycemic and antioxidant effects of a flavanone, naringenin, in streptozotocin–nicotinamide-induced experimental diabetic rats. *Journal of physiology and biochemistry* 2011; 68(3): 307–318.
14. Zatroch K, Knight C, Reimer J and Pang D. Refinement of intraperitoneal injection of sodium pentobarbital for euthanasia in laboratory rats (*Rattus norvegicus*). *BMC Vet Res.* 2016; 13: 60.
15. Bancroft J, Layton C. The Hematoxylin and eosin. In: Suvarna SK, Layton C and Bancroft JD. *Theory and Practice of histological techniques.* 7th ed. Churchill Livingstone of El Sevier, Philadelphia: Ch. 10 and 11; 2013; 172–214.
16. Hayat M. *Principles and Techniques of Electron Microscopy Biological Applications.* 4th ed. Macmillan Press, Scientific Medical LTD. London 2000; Pp. 522.
17. Kiernan J. *Histological and Histochemical Methods. Theory and Practice.* 4th ed., Butterworth-Heinemann. Oxford, Boston. Shock 2008; 12(6): 479.
18. Ramos-Vara JA, Kiupel M, Baszier T, Bliven L, Brodersen B, Chelack B. Suggested guidelines for immunohistochemical techniques in veterinary diagnostic laboratories. *J Vet Diagn Invest* 2008; 20: 393–413.
19. Dean A, Dean G, Colmbier D. *Epi-Info Version for the year 2000. Data Base, Statistics and Epidemiology on Microcomputer* CDC. Georgia, USA.
20. Yang Z, Li K, Yan X, Dong F, Zhao C. Amelioration of diabetic retinopathy by engrafted human adipose-derived mesenchymal stem cells in streptozotocin diabetic rats. *Graefes Archive for Clinical and Experimental Ophthalmology* 2010; 248(10): 1415-1422.
21. Kawano K, Hirashima T, Mori S, Saitoh Y, Kurosumi M, Natori T. Spontaneous long-term hyperglycemic rat with diabetic complications: Otsuka Long-Evans Tokushima Fatty (OLETF) strain. *Diabetes* 1992; 41:1422–1428.
22. Lu ZY, Bhutto IA, Amemiya T. Retinal changes in Otsuka long-evans Tokushima Fatty rats (spontaneously diabetic rat)–possibility of a new experimental model for diabetic retinopathy. *Japanese journal of ophthalmology* 2003; 47(1): 28-35.
23. Park SH, Park JW, Park SJ. Apoptotic death of photoreceptors in the streptozotocin-induced diabetic rat retina. *Diabetologia* 2003; 46: 1260–1268.
24. Enzsoly A; Szabo A, Kantor O, David C, Szalay P, Szabo K, Szel A, Nemeth J, Lukats A. Pathologic alterations of the outer retina in streptozotocin-induced diabetes. *Investigative ophthalmology and visual science* 2014; 55(6): 3686-3699.
25. Vujosevic S, Midena E. Retinal layers changes in human preclinical and early clinical diabetic retinopathy support early retinal neuronal and Müller cells alterations. *Journal of Diabetes Research* 2013; 1-8.
26. Kern TS, Berkowitz BA. Photoreceptors in diabetic retinopathy. *Journal of diabetes investigation* 2015; 6(4), 371-380.
27. Batenburg WW, Verma A, Wang Y. Combined renin inhibition/ (Pro) Renin receptor blockade in diabetic retinopathy- a study in transgenic (mREN2) 27 rats. *PLoS ONE* 2014; 9(6).
28. Cabrera DD, Somfai GM. Early detection of retinal thickness changes in diabetes using optical coherence tomography. *Medical Science Monitor* 2010; 16(3): 15-21.
29. Dijk VHW, Verbraak FD, Kok PH. Decreased retinal ganglion cell layer thickness in type 1 diabetic patients. *Investigative ophthalmology and visual science* 2010; 51(7): 3660-3665.
30. Krady JK, Basu A, Allen CM, Xu Y, LaNoue KF, Gardner TW, Levison SW. Minocycline reduces proinflammatory cytokine expression, microglial activation, and caspase-3 activation in a rodent model of diabetic retinopathy. *Diabetes* 2005; 54, 1559–1565.
31. Vincent JA, Mohr S. Inhibition of caspase-1/ interleukin-1 $\alpha$  signaling prevents degeneration of retinal capillaries in diabetes and galactosemia. *Diabetes* 2007; 56: 224–230.
32. El-Asrar AMA, Dralands L, Missotten L, Al-Jadaan IA, Geboes K. Expression of apoptosis markers in the retinas of human subjects with diabetes. *Investigative ophthalmology and visual science* 2004 45(8): 2760-2766.
33. Gaßtinger MJ, Kunselman AR, Conboy EE, Bronson SK, Barber AJ. Dendrite remodeling and other abnormalities in the retinal ganglion cells of Ins2 Akita diabetic mice. *Investigative ophthalmology and visual science* 2008; 49(6): 2635-2642.
34. Yong P H, Zong H, Medina RJ, Limb GA, Uchida K, Stitt AW, Curtis TM. Evidence supporting a role for N $\epsilon$ -(3-formyl-3, 4-dehydropiperidino) lysine accumulation in Müller glia dysfunction and death

- in diabetic retinopathy. *Molecular Vision* 2010; 16: 2524.
35. Curtis TM, Hamilton R, Yong PH, McVicar CM, Berner A, Pringle R, Stitt AW. Müller glial dysfunction during diabetic retinopathy in rats is linked to accumulation of advanced glycation end-products and advanced lipoxidation end-products. *Diabetologia* 2011; 54(3): 690-698.
  36. Takenaka K, Yamagishi S, Matsui T, Nakamura K, Imaizumi T. Role of advanced glycation end products (AGEs) in thrombogenic abnormalities in diabetes. *Neurovascular Research* 2006; 3(1): 73-77.
  37. Toma L, Stancu CS, Botez GM, Sima AV, Simionescu M. Irreversibly glycated LDL induce oxidative and inflammatory state in human endothelial cells; added effect of high glucose. *Biochemical and Biophysical Research Communication* 2009; 390(3): 877-882.
  38. Giunta S. Early changes in pituitary adenylate cyclase-activating peptide, vasoactive intestinal peptide and related receptors expression in retina of streptozotocin-induced diabetic rats. *Peptides* 2012; 37:32-39.
  39. Dijk VHW, Verbraak FD, Kok PH, Stehouwer M, Garvin MK, Sonka, Abramoff MD. Early Neurodegeneration in the Retina of Type 2 Diabetic Patients Retinal Neurodegeneration in Type 2 Diabetes. *Investigative ophthalmology and visual science* 2012; 53(6), 2715-2719.
  40. Mysona B, Dun Y, Duplantier J, Ganapathy V, Smith SB. Effects of hyperglycemia and oxidative stress on the glutamate transporters GLAST and system xc- in mouse retinal Müller glial cells. *Cell and Tissue Research* 2009; 335(3): 477-488.
  41. Li Q, Puro DG. Diabetes-induced dysfunction of the glutamate transporter in retinal Müller cells. *Investigative Ophthalmology and Visual Science* 2002; 43: 3109-3116.
  42. Berkowitz BA, Bissig D, Ye Y, Valsadia P, Kern TS, Roberts R. Evidence for diffuse central retinal edema in vivo in diabetic male Sprague Dawley rats. *PLoS One* 2012; 7(1): e29619.
  43. Mohammad G, Kowluru RA. Matrix metalloproteinase-2 in the development of diabetic retinopathy and mitochondrial dysfunction. *Laboratory Investigation* 2010; 90(9): 1365-1372.
  44. Wakabayashi Y, Usui Y, Okunuki Y. Correlation of vascular endothelial growth factor with chemokines in the vitreous in diabetic retinopathy. *Retina* 2010; 30: 339-344
  45. Seki M, Tanaka T, Nawa H, Usui T, Fukuchi T, Ikeda K, Takei N. Involvement of brain-derived neurotrophic factor in early retinal neuropathy of streptozotocin-induced diabetes in rats. *Diabetes* 2004; 53(9): 2412-2419.
  46. Tomita M, Adachi Y, Yamada H, Takahashi K, Kiuchi K, Oyaizu H, Ikebukuro K, Kaneda H, Matsumura M, Ikehara S. Bone marrow-derived stem cells can differentiate into retinal cells in injured rat retina. *Stem Cells* 2002; 20: 279-283.
  47. Ritter MR, Banin E, Moreno SK, Aguilar E, Dorrell MI, Friedlander M. Myeloid progenitors differentiate into microglia and promote vascular repair in a model of ischemic retinopathy. *Journal of Clinical Investigation* 2006; 116(12): 3266-3276.
  48. Rocco, DG, Iachininoto MG, Tritarelli A, Straino S, Zacheo A, Germani A, Crea, Capogrossi MC. Myogenic potential of adipose tissue-derived cells. *Journal of Cell Science* 2006; 119(14): 2945-2952.
  49. Liu Y, Yan X, Sun Z, Chen B, Han Q, Li J, Zhao RC. Flk-1+ adipose-derived mesenchymal stem cells differentiate into skeletal muscle satellite cells and ameliorate muscular dystrophy in mdx mice. *Stem Cells and Development* 2007; 16:695-706.
  50. Timper K, Seboek D, Eberhardt M, Linscheid P, Christ-Crain M, Keller U, Müller B, Zulewski H. Human adipose tissue derived mesenchymal stem cells differentiate into insulin, somatostatin, and glucagon expressing cells. *Biochemical and Biophysical Research Communications* 2006; 341(4): 1135-1140.
  51. Block GJ, Ohkouchi S, Fung F, Frenkel J, Gregory C, Pochampally R. Multipotent stromal cells are activated to reduce apoptosis in part by upregulation and secretion of stanniocalcin-1. *Stem cells* 2009; 27(3):670-681.
  52. Choi H, Lee RH, Bazhanov N, Oh JY, Prockop DJ. Anti-inflammatory protein TSG 6 secreted by activated MSCs attenuates zymosan-induced mouse peritonitis by decreasing TLR2/NF-kappa B signaling in resident macrophages. *Blood* 2011; 118:330-338.
  53. Kono TM, Sims EK, Moss DR, Yamamoto W, Ahn G. Human adipose-derived stromal/stem cells (hASCs) protect against STZ-induced hyperglycemia; analysis of hASC-derived paracrine effectors. *Stem Cells* 2014; 32(7): 1831-1842.

## الملخص العربي

دراسة بالميكروسكوب الضوئي والالكتروني عن الدور التحسيني المحتمل للخلايا الجذعية المشتقة من النسيج الدهني على إعتلال الشبكية السكري في ذكور الجرذان البيضاء البالغة

مجدي فتحي جاويش، نهاد فهمي مازن، إبتهاال زيد حسن، مي عيد عبدالهادي  
قسم الهستولوجيا و بيولوجيا الخلية - كلية الطب - جامعة الزقازيق

**المقدمة:** إن العلاج بالخلايا الجذعية له فعالية في علاج العديد من أمراض الانسان بما في ذلك اعتلال الشبكية. وقد ثبت انها آمنة وفعالة في مجموعة واسعة من الامراض المناعية.

**الهدف من العمل:** بحث التأثير الوقائي للخلايا الجذعية المشتقة من النسيج الدهني علي تلف شبكية العين بعد اعتلال الشبكية السكري المحدث.

**المواد وطرق البحث:** تم تقسيم أربعين من ذكور الجرذان إلى ثلاث مجموعات: المجموعة الأولى: قسمت إلى مجموعة ضابطة سلبية وإيجابية. المجموعة الثانية: حقنت داخل الصفاق بجرعة واحدة من عقار الاستربتوزوتوسين (٥٠ مجم/كجم) مذاب حديثا في ٩,٠% محلول ملح، وتم قياس مستوي الجلوكوز بالدم بعد يومين من استخدام العقار، واعتبرت الجرذان التي بلغت فيها نسبة الجلوكوز بالدم ٢٥٠ مجم بالمائة أو أكثر مصابة بالسكري واستخدمت في البحث. المجموعة الثالثة: تم حقنها بعقار الاستربتوزوتوسين كما في المجموعة السابقة ثم حقنت الجرذان المصابة بالسكري ب ٥,٠ مل من الخلايا الجذعية الدهنية (١×١٠<sup>٦</sup> خلية / مل)، معلقة في محلول فوسفات ملحي، في الوريد الذيلي. وبعد أربعة أسابيع تم إعداد عينات من الشبكية للدراسات الهستولوجية و الهستوكيميائية المناعية.

**النتائج:** أظهرت شبكية المجموعة المعالجة بالاستربتوزوتوسين ضعف الثنيات القاعدية للخلايا الشبكية الصغية وتشوه في الأقرص الرقائقية الخاصة بالجزء الخارجي للمستقبلات الضوئية، وفقدان للخلايا في الطبقة النووية الخارجية والداخلية والطبقة العقدية، وموت الخلايا المبرمج. وبعد اعطاء الخلايا الجذعية الدهنية وجد تحسن في تركيب الشبكية. و لوحظ انخفاض كبير في النسبة المئوية لمساحة تفاعل الكاسباز -٣ في جميع طبقات الشبكية، مقارنة مع مجموعة السكري. ولم يتم العثور على اختلاف بالمقارنة مع المجموعة الضابطة.

**الخلاصة:** إن العلاج بالخلايا الجذعية المشتقة من النسيج الدهني قد أثبتت فعاليته في الوقاية من اعتلال الشبكية السكري المحدث في الجرذان مما قد يمثل أداة قيمة للعلاج بالخلايا الجذعية في المستقبل.